Geoderma 439 (2023) 116688

Contents lists available at ScienceDirect

Geoderma

journal homepage: www.elsevier.com/locate/geoderma

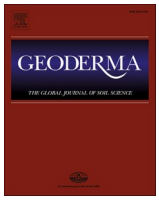

The divergent accumulation mechanisms of microbial necromass C in paddy soil under different long-term fertilization regimes

Li Xiong [a,b], Marios Drosos [c], Ping Wang [a,b], Wenxue Zhang [a,b], Wei Jin [d], Shaoxian Wang [a,b], Antonio Scopa [c], Zengbing Liu [a,b,*], Caihong Shao [a,b], Gang Sun [a,b], Kailou Liu [e]

[a] Institute of Soil and Fertilizer & Resources and Environment, Jiangxi Academy of Agricultural Sciences, Nanchang 330200, China
[b] National Engineering and Technology Research Center for Red Soil Improvement, Nanchang 330200, China
[c] Scuola di Scienze Agrarie, Forestali, Alimentari ed Ambientali, Universitá della Basilicata, Viale dell'Ateneo Lucano n. 10, Potenza 85100, Italia
[d] Agricultural Technology Promotion Center of Nanchang City, Nanchang 330009, China
[e] Jiangxi Institute of Red Soil and Germplasm Resources, Nanchang 331717, China

ARTICLE INFO

Handling Editor: Chaolei Yuan

Keywords:
Paddy soil
Microbial necromass
Long-term fertilization
Physical fractionation
Soil organic carbon

ABSTRACT

To investigate the stabilization mechanism of microbial necromass carbon (C) in rice paddy soil, the accumulation of microbial necromass and its contribution to SOC in bulk soil and in various fractions were addressed under a 40-year fertilization trial. The fertilization regimes included no fertilizer (Control), nitrogen, phosphorus and potassium inorganic fertilizer (NPK), and inorganic fertilizer plus manure (NPKM). Coarse particulate organic matter (cPOM), fine inter-microaggregate POM (fPOM), intra-microaggregate POM (iPOM), non-occluded silt plus clay fraction (s + c_f), and silt plus clay occluded within microaggregates (s + c_m) fractions were isolated. The results indicated that fungal necromass were the main component of microbial necromass across the fractions; however, the bacterial role was enhanced in mineral fractions (s + c_f and s + c_m) compared to POM fractions (cPOM, fPOM, and iPOM). The iPOM and mineral fractions stored more than 90 % of microbial necromass C due to the physical protection (organo-mineral associations and occlusion within microaggregates). Compared to Control, the significantly increased content of microbial necromass C and its contribution to SOC in bulk soil were attributed to the enhanced content of fungal necromass in iPOM fraction under NPK treatment. The highest content of microbial necromass C was found under NPKM treatment; moreover, the increased content of microbial necromass C in iPOM and s + c_m fractions made up to 82.80 % of that in bulk soil compared to Control, while a saturation behavior was found in s + c_f fraction. The contribution of microbial necromass to SOC was not altered under NPKM treatment compared to Control. However, a reduced fungal/bacterial necromass C ratio was found in bulk soil and iPOM fraction under NPKM treatment compared to Control, mainly due to the supply of higher quality substrates and the increased soil pH. As a whole, this study revealed the diverse responses of microbial necromass C accumulation and its contribution to SOC under different fertilization regimes in paddy soil.

1. Introduction

As a special type of anthropogenic soils (Anthrosols), paddy soils contain 18 Pg soil organic carbon (SOC) worldwide, accounting for 14 % of SOC pool in croplands (Liu et al., 2021a). This tremendous capacity of carbon (C) sequestration not only plays an important role in mitigating climate change (Xu et al., 2011), but also is crucial for ensuring the sustainability of paddy fields which produce one-fifth of world's energy consumption (Lal, 2004). Although microorganisms are the main driver of SOC transformation (Wiesmeier et al. 2019), their living biomass C makes up less than 4 % of SOC pool (Wei et al., 2022). Therefore, the microbial contribution to SOC was traditionally considered as low to negligible. Nevertheless, during the iterative process of cell growth, proliferation, and death, the microbial necromass can be continuously produced and accumulated in soils through the anabolism along with the utilization of plant-derived C (Liang et al., 2017). Recently, many studies on cropland soils suggested that the microbial necromass C accounted for around 50 % of SOC (Huang et al., 2019; Liang et al.,

* Corresponding author at: Jiangxi Academy of Agricultural Sciences, Nanchang 330200, China.
E-mail address: liuzengbing@163.com (Z. Liu).

https://doi.org/10.1016/j.geoderma.2023.116688
Received 13 December 2022; Received in revised form 9 October 2023; Accepted 10 October 2023

2019; Wang et al., 2021); however, the data were mostly collected from the upland soils.

As effective agronomic strategy, long-term fertilization, especially manure application, promoted the accumulation of microbial necromass in upland soils (Schmidt et al., 2015; Ye et al., 2019). However, the anaerobic environment in paddy fields could suppress microbial activities and oxidative enzymes production (Huang and Hall, 2017), consequently slowing down the microbial decomposition and transformation of plant residues. Chen et al. (2021) reported that the proportion of microbial necromass C in SOC was 28 %–36 % in paddy soils, which was significantly lower than that in adjacent upland soils (40 %–59 %). However, the relevant assessment of how the long-term fertilization regimes would affect the microbial necromass accumulation and whether its contribution to SOC in paddy soils would differ from those in upland soils is scarce.

In addition, SOC is a heterogeneous mixture with various biochemical fractions, which differs in decomposability and persistence (Haddix et al., 2020). Therefore, revealing the microbial necromass storage in different functional pools is the key to understand the microbial mechanism of C sequestration in paddy soils. Previous studies from upland soils suggested that mineral fractions were the main pool of microbial necromass (Lavallee et al., 2020; Wang et al., 2020), while contrary reports showed that more microbial necromass was stored in larger soil aggregates (Luan et al., 2021; Murugan et al., 2019). Moreover, Ding et al. (2017) suggested that the accumulation of microbial necromass in different fractions was clearly varied among the land use types. These inconsistent results indicate that further studies are required to explore the distribution pattern of microbial necromass among various SOC fractions and their responses to long-term fertilization regimes in rice paddy.

According to the degree of protection, Six et al. (2002a) proposed an effective procedure to isolate five SOC pools by physical fractionation, i.e., coarse particulate organic matter (cPOM), fine inter-microaggregate POM (fPOM), intra-microaggregate POM (iPOM), non-occluded silt plus clay fraction (s + c_f), and silt plus clay occluded within microaggregates (s + c_m). This approach was successfully used to study the response of C sequestration and stabilization to long-term fertilization practices (Huang et al., 2010; Yan et al., 2013). Amino sugars are regarded as microbial necromass biomarkers, and galactosamine (GlaN), glucosamine (GluN), and muramic acid (MurA) are the three most abundant amino sugars which can be quantified in soils (Amelung et al., 2008; Liu et al., 2021b). It is difficult to clarify from which organisms the GlaN has originated (Joergensen, 2018); however, the MurA exclusively originates from bacterial cell walls (Glaser et al., 2004). GluN mainly derives from the fungal chitin, although it can also be found in bacteria with a certain ratio to MurA (Appuhn and Joergensen, 2006; Engelking et al., 2007). In addition, the content of MurA and GluN contributes more than 60 % of the total amino sugars in soils (Joergensen, 2018). Therefore, the amount of MurA and GluN provides reliable information to evaluate the microbial necromass dynamics.

This study was conducted in a rice paddy with 40 years field experiment including inorganic fertilizer of nitrogen, phosphorus and potassium (NPK) and inorganic fertilizer plus manure (NPKM). The microbial necromass accumulation and its contribution to SOC in bulk soil and in various fractions were quantified. Since the varied substrate quality affects the substrate use efficiency of microbes (Cotrufo et al., 2013) and the different protection mechanisms of SOC (Huang et al., 2010) under different fertilization regimes, we hypothesized that (1) organic fertilization will generate a greater microbial necromass accumulation, especially for bacterial necromass compared to inorganic fertilization; (2) the responses of microbial necromass and its contribution to SOC in various fractions will be diverse under different long-term fertilization regimes. This study can give an insight into the stabilization mechanism of microbial necromass C in paddy soils.

2. Materials and methods

2.1. Site description

The field experiment was located at Zhanggong town in Jinxian county of Jiangxi province, China (28°21′ N, 116°10′ E). This area is prevailed under subtropical monsoon climate with mean annual rainfall of 1537 mm and mean annual temperature of 18.1 °C. According to IUSS (2006), the paddy soil is classified as Typic Stagnic Anthrosol derived from quaternary red clay dominated by kaolinites. The field experiment of long-term fertilization was initiated in 1981, and the soil properties of plough horizon (0–20 cm) before the experiment onset were: pH (H_2O) 6.9, SOC 16.22 g kg^{-1}, total N 1.49 g kg^{-1}, total P 0.48 g kg^{-1}, and total K 10.4 g kg^{-1} (Liu et al., 2019).

2.2. Experiment design and soil sampling

The paddy field is a double rice (*Oryza sativa* L.) cropping system comprising of early rice (April to July), late rice (July to November), and winter fallow from November to April of the next year. In the current study, three fertilization practices were selected from the field experiment: (1) unfertilized control (Control), (2) inorganic N, P, K fertilizers (NPK), and (3) inorganic N, P, K fertilizers plus organic manure (NPKM). The rate of fertilizer application was N 90.0 kg ha^{-1}, P 19.6 kg ha^{-1}, and K 60.9 kg ha^{-1} under NPK treatment for each rice season. The Chinese milk vetch (*Astragalus sinicus* L.) was applied in early rice season and the pig manure was applied in late rice season under NPKM treatment. The application rate was 22500 kg ha^{-1} (fresh weight) in each rice season for both types of organic manure. The basic properties of Chinese milk vetch were 70.6 % of water content, 467.0 g C kg^{-1}, 4.0 g N kg^{-1}, 1.1 g P kg^{-1}, and 3.5 g K kg^{-1} based on dry weight. These properties of pig manure were 85.5 % of water content, 340.0 g C kg^{-1}, 6.0 g N kg^{-1}, 4.5 g P kg^{-1}, and 5.0 g K kg^{-1} (Yan et al., 2022). The input of N, P, and K under NPKM treatment was the same with NPK treatment. 60 % of N, 100 % of P, 50 % of K, and 100 % of organic manure were applied before the rice seedling transplantation as the basal fertilizer. The remaining N and K were topdressed at tillering stage (about 10 days after transplantation). The tillage practice, weed control, water irrigation and pesticide application were consistent across the treatments. The fertilization rates and agronomic production were maintained since 1981 when this field experiment was initiated. The grain yield of different fertilization regimes is shown in Fig. S1.

Each treatment comprised of three replicates in a randomized block design with 46.67 m^2 for each replicated plot. Water and nutrients exchange between the plots was prevented by concrete frames with 10 cm width. The soil samples were collected from the plots in December 2020 after the late rice harvest. Six random cores (4 cm in diameter) were taken from the plough horizon (0–20 cm) and mixed to create a composite sample at each plot. Soil samples were sieved through a 2-mm sieve. All stones, plant roots and debris were removed with tweezers, and then the soil samples were air-dried at room temperature for analysis.

2.3. SOC physical fractionation

The method suggested by Six et al. (1998; 2002a) was performed to isolate different SOC fractions (Fig. S2). Briefly, 50 g of < 2 mm bulk soil were placed on a 250-μm sieve, and were then shaken with 50 glass beads (4 mm diameter) to break up macroaggregates. With the help of a continuous and steady water flow, the microaggregates were flushed onto a 53-μm sieve to avoid further disruption by the beads. After complete macroaggregates breakup, any material retained on the 250-μm sieve, except the beads, was coarse particulate organic matter (cPOM). Then wet-sieving was conducted to separate the rest portion into microaggregates (>53 μm) and non-occluded silt plus clay fraction (s + c_f) (<53 μm).

Microaggregates were further isolated into three fractions by density fractionation after oven-dried at 50 °C. A 5 g subsample of microaggregates was added into a 50 ml centrifuge tube with 35 ml of 1.85 g cm^{-3} sodium iodide (NaI), and the tube was shaken reciprocally by hand for around 30 times. Another 10 ml of NaI solution was used to wash down the remaining material on cap and sides of centrifuge tube, and then the tube was put in a vacuum chamber for 10 min. After 20 min equilibration, the sample was centrifuged (1250 × g for 60 min), and the supernatant was aspirated onto a 20-μm sieve and was completely rinsed with deionized water to obtain fine inter-microaggregate POM (fPOM). After rinsing twice with 50 ml of deionized water, 30 ml of 0.5 % sodium hexametaphosphate was used to disperse the microaggregates by shaking for 18 h. The dispersed microaggregates were then isolated into intra-microaggregate POM (iPOM) (>53 μm) and silt plus clay fraction occluded within microaggregates (s + c_m) (<53 μm) by wet-sieving. Finally, the cPOM, fPOM, iPOM, s + c_f, and s + c_m fractions were dried at 50 °C, weighted and stored for analysis.

2.4. Amino sugars analysis

According to Zhang and Amelung (1996), after passing through a 150-μm sieve, the dried soil sample containing ≥0.3 mg N was hydrolyzed in 10 ml of HCl (6 M) for 8 h at 105 °C. 100 μl of internal standard (myo-inositol) were added, and the hydrolysate was filtered, adjusted to pH 6.6–6.8 with KOH (1 M) and HCl (0.01 M), centrifuged (3000×g for 15 min), and dried by rotary evaporation. The residue was washed into a 3 ml vial with methanol, dried by N_2 gas, re-dissolved in 1 ml of deionized water and 100 μl of quantitative standard (N-methylglucamine), was then frozen, and lyophilized. For the aldononitrile derivatives preparation, 32 mg ml^{-1} of hydroxylamine hydrochloride and 40 mg ml^{-1} of 4-(dimethylamino)-pyridine in pyridine-methanol (volume ratio of 4/1) were used to obtain the derivatization reagent. Then the lyophilized residue was dissolved in 300 μl of this reagent and was water-bathed at 75–80 °C for 35 min. After cooling, 1 ml of acetic anhydride was added into the solution and was water-bathed at the same temperature for 25 min. Cooled again, 1.5 ml of dichloromethane and 1 ml of HCl (1 M) were successively added into the solution, and were then vortexed at 25 °C for 30 s. Excess derivatization reagents were thoroughly washed using 1 ml of deionized water three times. The amino sugar derivatives were concentrated by drying with N_2 gas, and were then re-dissolved in 300 μl of hexane–ethyl acetate solvent (volume ratio of 1/1) for determination. Three amino sugars, i.e., GluN, MurA, and GlaN, were measured using a gas chromatograph equipped with a flame ionization detector (Agilent 7890B GC, Agilent Technologies) and an HP-5 fused silica column (30 m × 0.25 mm × 0.25 μm).

As described by Appuhn and Joergensen (2006) and Engelking et al. (2007), Fungal GluN, an index for fungal necromass, was estimated by subtracting bacterial GluN from total GluN, assuming that MurA and GluN occur at a molar ratio of 1/2 in bacterial cells. MurA is the index for bacterial necromass. Thus, Fungal and bacterial necromass C (g kg^{-1}) were calculated using Eqs. (3) and (4), respectively:

$$\text{Fungal necromass C} = [\text{mol GluN} - (2 \times \text{mol MurA})] \times 179.2 \times 9 \quad (3)$$

$$\text{Bacterial necromass C} = \text{MurA} \times 45 \quad (4)$$

where 179.2 is the molecular weight of GluN and 9 is the conversion value of fungal GluN to fungal necromass C in Eqs. (3). 45 is the conversion value of MurA to bacterial necromass C in Eqs. (4). Total microbial necromass C was the sum of fungal and bacterial necromass C. The proportion of microbial necromass C in SOC indicated the microbial contribution to SOC accumulation. The relative contribution of fungal and bacterial necromass C in SOC sequestration was evaluated by the fungal/bacterial necromass C ratio. However, the main limitations of converting amino sugars to microbial necromass C should be declared. Firstly, the conversion values deriving from the pure culture may change for microbes under different starvation conditions (Liang et al., 2019). Secondly, the calculation based on amino sugars ignores the contribution of microbial extracellular products to SOC (Costa et al., 2018). Additionally, the extraction efficiency and detection of amino sugars could vary with different substrates (Liang, 2020). Even so, amino sugars biomarker analysis is a widely used and accepted method due to the absence of a more appropriate alternative.

2.5. Soil chemical properties determination

Soil pH was measured using a glass electrode (soil/water ratio of 2/5, m/v) with a PHS-3BW pH meter (Lu, 2000). The concentration of SOC and total N in bulk soil and in various fractions was measured by dry combustion analysis in an elemental analyzer (Vario MACRO cube, Elementar) without HCl pre-treatment since no carbonate C was found in these acidic soils.

2.6. Statistical analysis

The recovery rates of SOC, total N, and amino sugars were calculated as follows:

$$\text{Recovery rate } (\%) = \Sigma\ (A_{fraction} \times M_{fraction}) \ / \ A_{soil} \times 100$$

Where $A_{fraction}$ was the concentration of SOC, total N, and amino sugars in each fraction; $M_{fraction}$ was the mass proportion of each fraction; and A_{soil} was the concentration of SOC, total N, and amino sugars in bulk soil. The content of SOC, total N, and microbial necromass C in each fraction was the result of $A_{fraction} \times M_{fraction}$, which reflected the change of pool size in various fractions. One-way ANOVA was used to assess the effect of fertilization treatments on soil chemical and microbial properties in bulk soil. The differences of these soil properties among various fractions within a fertilization treatment and among the treatments within a fraction were analyzed with one-way MANOVA. All data were examined for normality and homogeneity of variances, and were ln-transformed when necessary. The least significant difference (LSD) was used to identify the statistical significance at $P < 0.05$. The linear regression and coefficient of determination were adopted to depict the relationship between the soil properties and the microbial variables. All data were expressed as mean ± SD. The statistical analysis was carried out by SPSS 20.0 and the figures were made by Origin 8.0.

3. Results

3.1. Effect of long-term fertilization on soil chemical properties in bulk soil

As shown in Fig. 1, the SOC content in bulk soil was significantly increased from 18.90 g kg^{-1} to 24.53 g kg^{-1} under NPKM treatment compared with Control; while no significant change was detected under NPK treatment. Similar trend was noticed for total N content (Table S1). Compared to Control, NPK treatment significantly increased the C/N ratio from 9.51 to 9.90; however, NPKM treatment decreased it to 9.05. The soil pH of 5.22 was observed under Control and a significant increase was only found under NPKM treatment (Fig. 1).

3.2. Effect of long-term fertilization on mass proportion, SOC content, and C/N ratio in various fractions

The recovery rate of fractionation process under different treatments ranged from 94.38 % to 98.18 % (Table 1). The mass proportion of various fractions followed the order: s + c_m > s + c_f > iPOM > cPOM > fPOM across the treatments. Compared to Control, NPKM treatment significantly increased the proportion of cPOM and fPOM fractions, while decreased that of s + c_m fraction. No significant change was found under NPK treatment except an increase in fPOM fraction (Table 1).

After fractionation, the recovery rate of SOC ranged from 97.37 % to

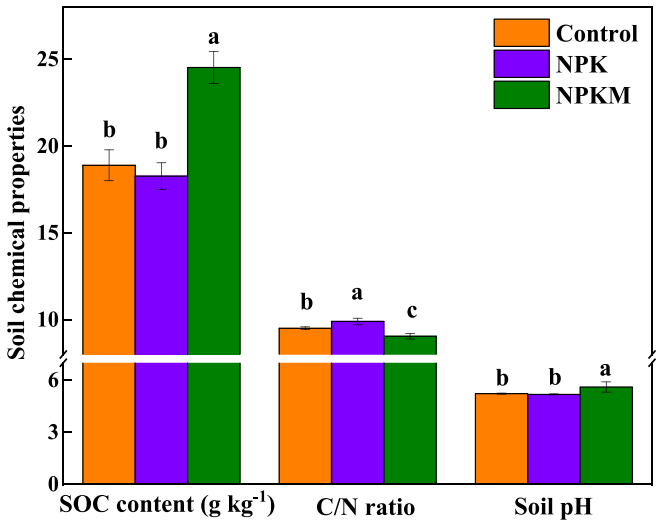

Fig. 1. SOC content, C/N ratio, and pH in bulk soil under long-term fertilization treatments. Different lowercase letters indicate significant difference among fertilization treatments (Fisher's LSD test, $P < 0.05$). Control: no fertilizer application; NPK: N, P, and K fertilizer application; NPKM: N, P, and K fertilizer with manure application.

103.41 %. The major SOC pools were s + c_m, s + c_f and iPOM fractions (Table 1), accounted for more than 85 % of SOC in bulk soil irrespective of the treatments (Table S2). Compared to Control, NPKM treatment significantly increased the SOC content in all fractions except in s + c_f; however, no significant change was detected in any fractions under NPK treatment (Table 1). Similar results were found for total N content (Table S1, Table S2).

The C/N ratio in POM fractions (cPOM, fPOM, and iPOM) was significantly higher than that in mineral fractions (s + c_f and s + c_m) (Table 1). Compared to Control, NPK treatment significantly increased the C/N ratio in fPOM, iPOM, and s + c_m fractions by 14.89 %, 15.61 %, and 16.48 %, respectively. However, NPKM treatment only decreased it in fPOM fraction (Table 1).

3.3. Effect of long-term fertilization on the content of microbial necromass C in bulk soil and in various fractions

The content of total microbial, fungal, and bacterial necromass C in bulk soil was 8.85 g kg^{-1}, 6.47 g kg^{-1}, and 2.38 g kg^{-1}, respectively, under Control (Fig. 2A-C). All the fertilization practices significantly increased these microbial properties in bulk soil except the bacterial necromass C under NPK treatment (Fig. 2C). Compared to Control, NPKM treatment significantly increased the content of total microbial, fungal, and bacterial necromass C in all fractions except in s + c_f (Fig. 2A-C). NPK treatment significantly enhanced the content of total microbial and fungal necromass C in all POM fractions (Fig. 2A-B) and the content of bacterial necromass C in fPOM fraction (Fig. 2C). Moreover, a greater enhancement was found under NPKM compared with NPK treatment.

Although the greatest concentration of microbial necromass C was found in fPOM fraction (Table S3), the highest content of microbial necromass C was invariably detected in s + c_m fraction across the treatments (Fig. S3A-C). And the content of total microbial, fungal, and bacterial necromass C in iPOM and s + c_f fractions was significantly higher than that in cPOM and fPOM fractions (Fig. S3A-C). About 70 % of microbial necromass C was distributed in s + c_m and s + c_f fractions, and iPOM stored more than 20 % of microbial necromass C regardless of the treatments (Table 2). Fertilization practices did not significantly change the proportion of microbial necromass C in the three major pools (iPOM, s + c_f, and s + c_m fractions) except a significant reduction of bacterial necromass C in s + c_f under NPKM compared to NPK treatment (Table 2).

3.4. Effect of long-term fertilization on fungal/bacterial necromass C ratio and microbial contribution to SOC in bulk soil and in various fractions

As to the fertilization effect, only NPKM treatment significantly decreased the fungal/bacterial necromass C ratio from 2.72 to 2.38 in bulk soil and from 2.96 to 2.29 in iPOM fraction compared with Control (Fig. 3). The fungal/bacterial necromass C ratio basically declined, following the order: cPOM > fPOM > iPOM > s + f_m ≈ s + c_f across the treatments, although a significant difference was not consistent among the fractions (Fig. S4).

Compared to Control, the contribution of microbial necromass C to SOC in bulk soil was significantly increased from 46.80 % to 54.20 % under NPK treatment, while no significant change was found under NPKM treatment (Fig. 4). NPK treatment significantly increased the microbial contribution to SOC in fPOM and iPOM fractions; while, NPKM treatment increased the microbial contribution only in fPOM fraction (Fig. 4). The contribution of microbial necromass C to SOC in various fractions generally followed the order: s + c_m > s + c_f > iPOM > fPOM > cPOM (Fig. S5).

3.5. Correlation of SOC in bulk soil and microbial necromass C in bulk soil and in various fractions

The SOC content in bulk soil was positively correlated with the total microbial necromass C in bulk soil, cPOM, fPOM, iPOM, and s + c_m fractions (Fig. 5A-B). Similar result was found for fungal and bacterial necromass C (Fig. 5C-F) except for the fungal necromass C in iPOM

Table 1
Mass proportion, SOC content, and C/N ratio of various fractions under long-term fertilization treatments (mean ± SD, n = 3).

	Treatment	cPOM	fPOM	iPOM	s + c_f	s + c_m	Recovery (%)
Mass proportion (%)	Control	3.74 ± 0.23 Bd	0.59 ± 0.10 Ce	12.86 ± 2.45 c	34.57 ± 2.34 b	46.43 ± 1.57 Aa	98.18 ± 1.52
	NPK	4.07 ± 0.18 Bd	1.04 ± 0.04 Be	12.84 ± 1.79 c	33.73 ± 2.90 b	44.85 ± 0.54 ABa	96.53 ± 1.20
	NPKM	4.55 ± 0.12 Ad	1.52 ± 0.21 Ae	15.54 ± 0.52 c	30.21 ± 2.42 b	42.56 ± 2.81 Ba	94.38 ± 0.62
SOC content (g kg^{-1} soil)	Control	0.92 ± 0.12 Bc	0.71 ± 0.11 Bc	5.12 ± 0.94 Bb	4.68 ± 0.43 b	6.97 ± 0.65 Ba	97.37 ± 3.52
	NPK	1.11 ± 0.17 Bc	0.93 ± 0.08 Bc	5.26 ± 0.70 Bb	4.39 ± 0.36 b	7.21 ± 0.51 ABa	103.41 ± 2.74
	NPKM	1.90 ± 0.25 Ac	2.17 ± 0.17 Ac	7.84 ± 0.22 Aa	4.66 ± 0.23 b	8.40 ± 0.61 Aa	101.81 ± 1.93
C/N ratio	Control	18.05 ± 1.77 a	14.60 ± 0.42 Bb	10.04 ± 0.62 Bc	8.61 ± 0.15 d	7.20 ± 0.75 Be	
	NPK	16.70 ± 0.57 a	16.77 ± 1.05 Aa	11.61 ± 0.90 Ab	8.24 ± 0.57 c	8.38 ± 0.12 Ac	
	NPKM	16.42 ± 1.89 a	10.02 ± 0.20 Cb	10.05 ± 0.61 Bb	8.33 ± 0.19 c	7.46 ± 0.21 Bc	

Different uppercase letters in a single column indicate significant difference among fertilization treatments in a fraction; different lowercase letters in a single row indicate significant difference among fractions under each fertilization treatment (Fisher's LSD test, $P < 0.05$). No letter indication stands for non-significant difference among fertilization treatments or various fractions. POM, particulate organic matter; cPOM, coarse POM; fPOM, fine inter-microaggregate; iPOM, intra-microaggregate POM; s + c_f, non-occluded silt plus clay fraction; s + c_m, silt plus clay occluded within microaggregates. Control: no fertilizer application; NPK: N, P, and K fertilizer application; NPKM: N, P, and K fertilizer with manure application.

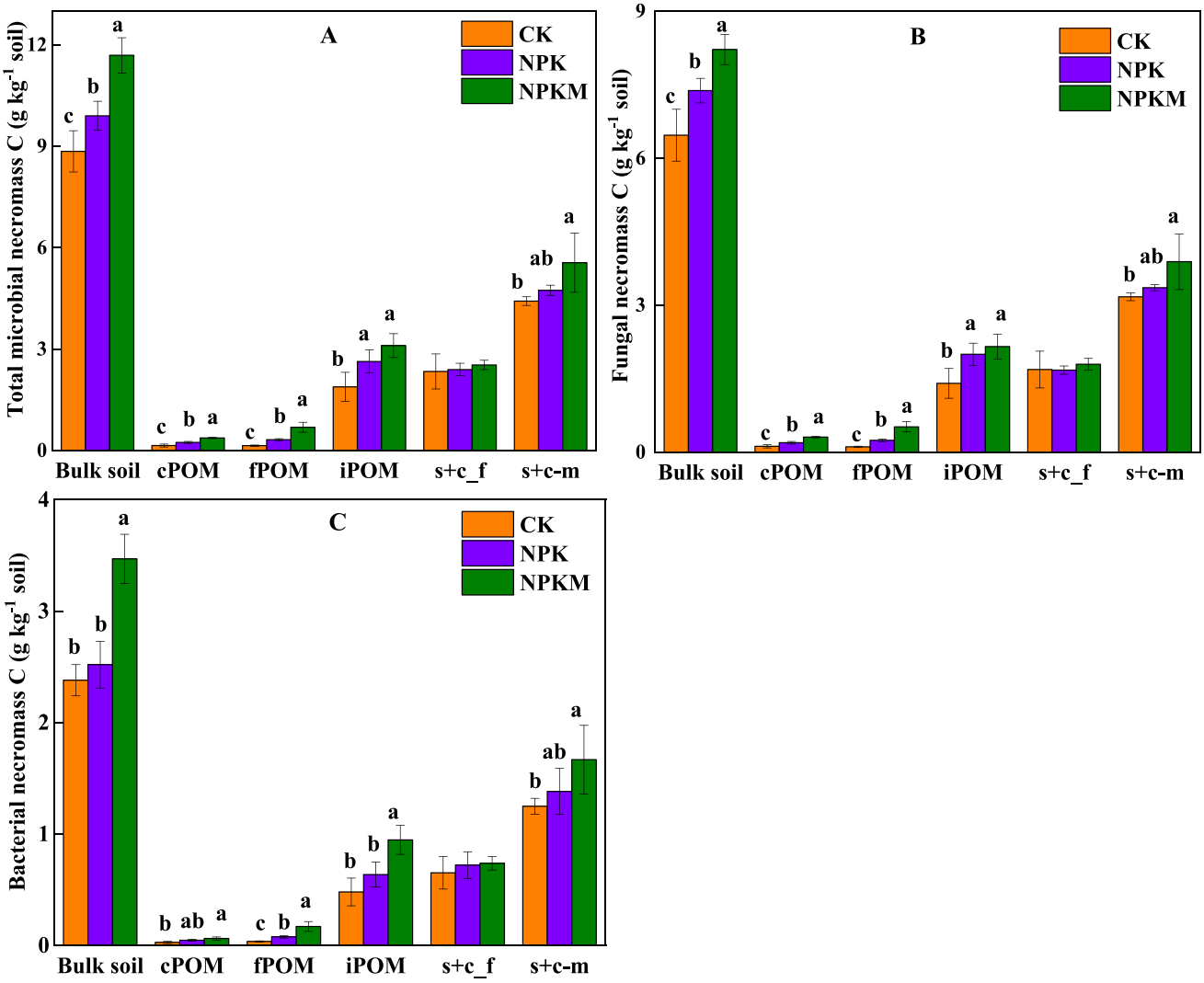

Fig. 2. Content of total microbial (A), fungal (B), and bacterial (C) necromass C in bulk soil and fractions under long-term fertilization treatments. Different lowercase letters indicate significant difference among fertilization treatments in bulk soil and fractions (Fisher's LSD test, $P < 0.05$). No letter indication stands for non-significant difference among fertilization treatments. POM, particulate organic matter; cPOM, coarse POM; fPOM, fine inter-microaggregate POM; iPOM, intra-microaggregate POM; s + c_f, non-occluded silt plus clay fraction; s + c_m, silt plus clay occluded within microaggregates.

(Fig. 5D). Interestingly, no significant linear relationship was found between SOC in bulk soil and microbial necromass C in s + c_f fraction (Fig. 5A, C, E).

4. Discussion

4.1. Microbial necromass C accumulation across the various fractions

Similar to previous studies in paddy fields (Liu et al., 2021; Luo et al., 2021), fungal necromass accounted for more than 70 % of the total microbial necromass C in bulk soil and in various fractions irrespective of the treatments (Fig. 2A-C). The fungal/bacterial necromass C ratio, ranging from 2.36 to 5.13, also proved the fungal dominance in microbial necromass C accumulation (Fig. 3). This phenomenon mainly resulted from a greater C-use efficiency of fungi compared with bacteria (Adu and Oades, 1978) and a higher resistance of fungal necromass to microbial decomposition due to the more recalcitrant components like chitin (Kögel-Knabner, 2002). Chen et al. (2018) also suggested that fungal dominance enhanced along the trial progress in newly formed microbial necromass conducted within a paddy soil. However, the descending order of fungal/bacterial necromass C ratio among the various fractions (Fig. S4) indicated an enhanced bacterial role in microbial necromass accumulation in mineral fractions relative to POM. POM, especially unprotected cPOM and fPOM, mainly comprised of fresh and decomposing plant residues with a higher C/N ratio compared to mineral fractions (Table 1). Therefore, as the main decomposer of plant materials, fungi showed an advantage in utilization and decomposition of POM fractions (Hendrix et al., 1986; Neely et al., 1991). Previous study reported that more POM content enhanced the soil porosity (Schlüter et al., 2022), which could promote the fungal hyphae elongation (Harris et al., 2003). Angst et al. (2021) also suggested the significantly enhanced bacterial necromass role in mineral fractions compared to macro- and microaggregates, which were mainly occluded or associated with the POM fractions.

The mineral fractions distributed around 70 % of microbial necromass C (Table 2) and displayed a higher microbial contribution to SOC compared to POM fractions (Fig. S5). These results indicated that microbial necromass could be preferentially stored in mineral fractions (Lavallee et al., 2020; Wang et al., 2020), leading to a lower C/N ratio (Table 1). The primary mechanism was the large specific surface areas and the hydroxyl groups' site density in mineral fractions, which enhanced the affinity of microbial necromass and reduced its decomposition rate (Churchman, 2018; Lehmann et al., 2008; von Lützow et al., 2008). Moreover, the iPOM fraction stored more than 20 % of

Table 2
Proportion (%) of total microbial, fungal, and bacterial necromass C in various fractions under long-term fertilization treatments (mean ± SD, n = 3).

	Treatment	cPOM	fPOM	iPOM	s + c_f	s + c_m
Total microbial necromass C	Control	1.65 ± 0.38 Cc	1.64 ± 0.33 Cc	21.55 ± 5.96 b	26.26 ± 4.12 b	50.18 ± 4.76 a
	NPK	2.42 ± 0.27 Bc	3.23 ± 0.37 Bc	26.72 ± 4.58 b	24.18 ± 1.41 b	47.96 ± 3.71 a
	NPKM	3.18 ± 0.25 Ad	5.92 ± 1.54 Ac	26.56 ± 3.09 b	21.69 ± 1.79 b	47.39 ± 5.54 a
Fungal necromass C	Control	1.85 ± 0.40 Cc	1.70 ± 0.35 Cc	22.00 ± 5.93 b	25.88 ± 3.73 b	49.31 ± 5.02 a
	NPK	2.61 ± 0.29 Bc	3.29 ± 0.42 Bc	27.15 ± 4.01 b	22.68 ± 0.38 b	45.50 ± 1.06 a
	NPKM	3.76 ± 0.33 Ad	6.33 ± 1.53 Ac	26.26 ± 3.53 b	21.86 ± 2.22 b	47.18 ± 5.43 a
Bacterial necromass C	Control	1.12 ± 0.34 Bc	1.48 ± 0.28 Cc	20.39 ± 6.22 b	27.34 ± 5.20 ABb	52.59 ± 4.05 a
	NPK	1.88 ± 0.46 Ac	3.04 ± 0.41 Bc	25.52 ± 6.39 b	28.68 ± 5.11 Ab	55.51 ± 13.15 a
	NPKM	1.79 ± 0.32 ABe	4.95 ± 1.59 Ad	27.27 ± 2.48 b	21.26 ± 1.01 Bc	47.89 ± 5.79 a

Different uppercase letters in a single column indicate significant difference among fertilization treatments in a fraction; different lowercase letters in a single row indicate significant difference among fractions under each fertilization treatment (Fisher's LSD test, $P < 0.05$). No letter indication stands for non-significant difference among fertilization treatments or various fractions.

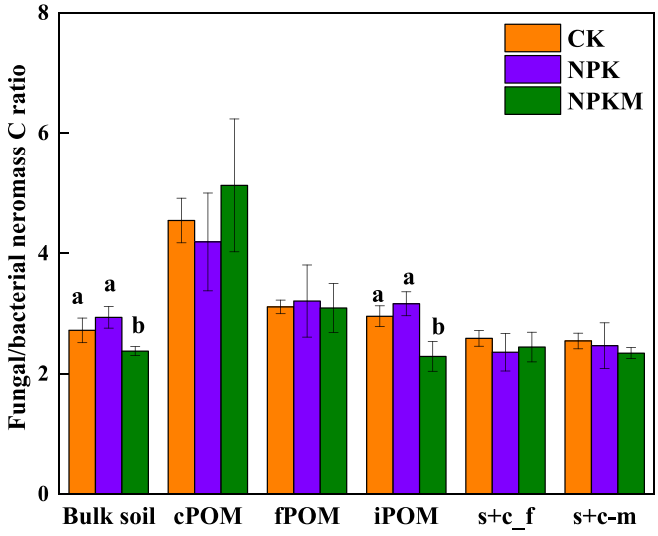

Fig. 3. Fungal/bacterial necromass C ratio in bulk soil and fractions under long-term fertilization treatments. Different lowercase letters indicate significant difference among fertilization treatments in bulk soil and fractions (Fisher's LSD test, $P < 0.05$). No letter indication stands for non-significant difference among fertilization treatments.

microbial necromass being comparable to the proportion in s + c_f across the treatments (Table 2) mainly due to the occlusion within microaggregates. This mechanism could also lead to the greater proportion of microbial necromass C in s + c_m fraction compared with s + c_f (Table 2). Our results suggested that the physical protection (organo-mineral associations and occlusion within microaggregates) plays a substantial role in microbial necromass accumulation in paddy soil, which was defined as the entombing effect by Liang et al. (2017).

4.2. *Effect of inorganic fertilization on microbial necromass C accumulation and its contribution to SOC across the various fractions*

As the main contributor of the increased total microbial necromass, the enhancement of fungal necromass was found in POM fractions with 40 years of inorganic fertilization (Fig. 2A-B); however, the increased bacterial necromass was found only in fPOM fraction (Fig. 2C). Although rice straw was removed from the plots after every harvest, inorganic fertilization could increase the root biomass inferred from the enhanced grain yield (Fig. S1). The complex components and high C/N ratio of root-derived C could benefit fungal utilization over bacteria (Bai et al., 2013; Barreiro et al., 2016), resulting in a greater fungal necromass accumulation. Meanwhile, the root materials were the main source of POM (Six et al., 2002b), which was not well associated with the mineral fractions (Tong et al., 2014). As a result, no significant change of microbial necromass was observed in mineral fractions under inorganic fertilization (Fig. 2A-C). In addition, the nutrient ions from inorganic fertilizer could lead to the desorption of organic compounds like amino sugars due to the competitive sorption (Greenland, 1971; Schneider et al., 2010), which might also limit the enhancement of microbial necromass in mineral fractions. Future research may reveal the detailed mechanism, which has not been yet well reported. Furthermore, the increased fungal necromass C in iPOM fraction accounted for 64.87 % of that in bulk soil (Fig. 2B). This could be attributed to a slower turnover rate of microbial necromass due to the physical occlusion within microaggregates (Six et al., 2002a). Therefore, the current study suggested that the increase in fungal nercomass in iPOM fraction was the main driver for the microbial necromass accumulation in paddy soil with inorganic fertilization. Although long-term inorganic fertilization significantly increased the living bacterial biomass in paddy soils (Dai et al., 2017; Dong et al., 2014), no significant increase of bacterial necromass C was found except in fPOM (Fig. 2C). The inorganic fertilization, especially the application of N and P fertilizers, could shift the microbial P limitation to C limitation (Luo et al., 2020). Therefore, the accelerated decomposition of bacterial necromass could occur to compensate for the microbial C demand due to the weaker resistance of bacterial necromass (Kögel-Knabner, 2002; Luo et al., 2021).

However, the positive effect of inorganic fertilization on total microbial and fungal necromass C accumulation (Fig. 2A-B) did not alter the SOC content in bulk soil and its various fractions (Table 1), in agreement with the reports from the same experimental field (Huang et al., 2010; Yan et al., 2022). These results implied that inorganic fertilization relieved N limitation and accelerated the decomposition of plant component in POM fractions through shifting the stoichiometry of inputs closer to meet the microbial N demand (Lavallee et al., 2020). Consequently, the enhanced microbial contribution to SOC was found in bulk soil, fPOM, and iPOM fractions (Fig. 4).

4.3. *Effect of organic fertilization on microbial necromass C accumulation and its contribution to SOC across the various fractions*

Due to greater C input, the significant enhancement of microbial necromass C was found in bulk soil and in various fractions except in s + c_f with organic fertilization (Fig. 2A-C). Specifically, the increase of total microbial necromass C in iPOM and s + c_m fractions accounted for 82.80 % of the enhanced total microbial necromass C and for 41.83 % of the enhanced SOC in bulk soil, respectively (Fig. 2A and Table 1). Therefore, the accumulation of microbial necromass in iPOM and s + c_m fractions was the key driver for microbial necromass stabilization and SOC sequestration in paddy soil with organic fertilization due to the physical protection of microaggregates.

The total microbial, fungal, and bacterial necromass C did not significant change in s + c_f fraction with organic fertilization (Fig. 2A-C),

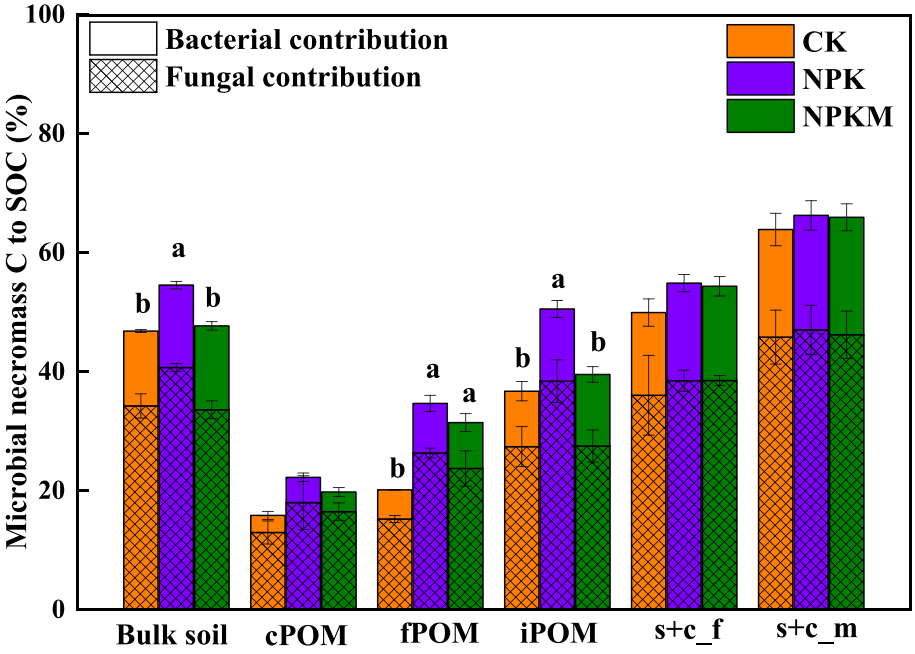

Fig. 4. Contribution of microbial necromass C to SOC in bulk soil and fractions under long-term fertilization treatments. Different lowercase letters indicate significant difference among fertilization treatments in bulk soil and fractions (Fisher's LSD test, $P < 0.05$). No letter indication stands for non-significant difference among fertilization treatments.

which could be related to the saturation behavior of this fraction. As shown in Fig. 5A-B, SOC content in bulk soil was positively correlated with the total microbial necromass C in bulk soil and in all the fractions except in s + c_f. Many studies used SOC content as the proxy of C input to estimate the saturation behavior of various fractions (Stewart et al., 2008; Yang et al., 2018). Thus, these results indicated that the paddy soil still has a potential to sequester more microbial necromass C, although s + c_f fraction reached the saturation level. According to the hierarchical C saturation theory, the mineral fractions could reach the saturation level before the POM fractions (Castellano et al., 2015; Kool et al., 2007; Stewart et al., 2009). Interestingly, an unsaturated phenomenon was found in s + c_m fraction, which was contrary to s + c_f fraction (Fig. 5A, C, E). Sokol et al. (2018) suggested that the direct sorption of low molecular weight OC, mainly dissolved OC, was a non-negligible pathway for mineral associated OC formation. Moreover, the dissolved OC generated from manure contained more high polar compounds, such as phenolic groups, which exhibited strong sorptive affinity for mineral surfaces (Zhang et al., 2021), but were inefficiently biosynthesized by microbes (Frey et al., 2013). Therefore, the dissolved OC could much easier be adsorbed directly to s + c_f compared with s + c_m due to the physical occlusion within microaggregates, limiting the association of microbial necromass with s + c_f due to competitive adsorption. The significant lower contribution of microbial necromass to SOC in s + c_f compared to s + c_m strongly proved this mechanism (Fig. S5). The saturation behavior was found for fungal necromass C in iPOM fraction (Fig. 5D) but not for the bacterial necromass C (Fig. 5F); the exact reason is unknown since this phenomenon was insufficiently reported. The differential stabilization mechanism might be one explanation, considering their possibly different intrinsic stability (He et al., 2011). In addition, the poor aeration within microaggregates could be another reason along with the limited fungal growth (Sey et al., 2008).

The microbial contribution to SOC was unaltered in bulk soil and in various fractions except in fPOM with organic fertilization (Fig. 4). In fact, this contribution even decreased in bulk soil and iPOM fraction in relation to inorganic fertilization. Organic fertilization, such as manure application, would increase the input of non-microbial organic debris (Li et al., 2020; Xia et al., 2021). Considering the increased SOC content (Table 1), these results implied a synchronous accumulation of microbial- and plant-derived C with organic fertilization. A significant decrease in fungal/bacterial necromass C ratio was found in bulk soil and iPOM fraction (Fig. 3), reflecting an accrual of bacterial necromass with organic fertilization. Firstly, manure addition supplied higher quality substrates (lower C/N ratio), which could be utilized by bacteria more easily (Guggenberger et al., 1999). In addition, the enhanced soil pH (Fig. 1) could stimulate bacterial growth and increase its necromass accumulation, according to the positive correlation between bacterial necromass C and soil pH (Fig. S6). Although the optimum pH range for bacterial growth is narrower than for fungi, the pH increase is positive for bacterial growth in arable soil within the gradient of 4.0–8.3 (5.16–5.92 in the current study, Fig. 1) (Rousk et al., 2009). Furthermore, the reduced fungal/bacterial necromass C ratio in iPOM could be attributed to the saturation behavior of fungal necromass (Fig. 5D), which limited the further increase of fungal necromass. In addition, the unsaturation of bacterial necromass indicated that iPOM has the capacity to sequester more bacterial necromass with the enhancement of C input (Fig. 5F).

5. Conclusions

Our research showed that the microbial necromass C accumulation was mainly driven by fungi in bulk soil and its various fractions in paddy field regardless of the fertilization treatments. Physical protection controlled the microbial necromass C accumulation, since around 90 % of the microbial necromass was detected in mineral (s + c_f and s + c_m) and iPOM fractions. The higher increase in microbial necromass C, just like hypothesized, was found under organic fertilization compared to inorganic treatment. Moreover, the accumulation mechanisms of microbial necromass C varied in paddy soil under different fertilization regimes. The enhancement of fungal nercomass in iPOM fraction was the key to increase microbial necromass C under inorganic fertilization; however, the main increase of microbial necromass C was found in iPOM and s + c_m fractions under organic fertilization. It is notable that the saturation behavior of microbial necromass was found in s + c_f fraction under organic fertilization. Furthermore, inorganic fertilization increased the microbial contribution to SOC due to the enhanced accumulation of microbial necromass and decomposition of plant-

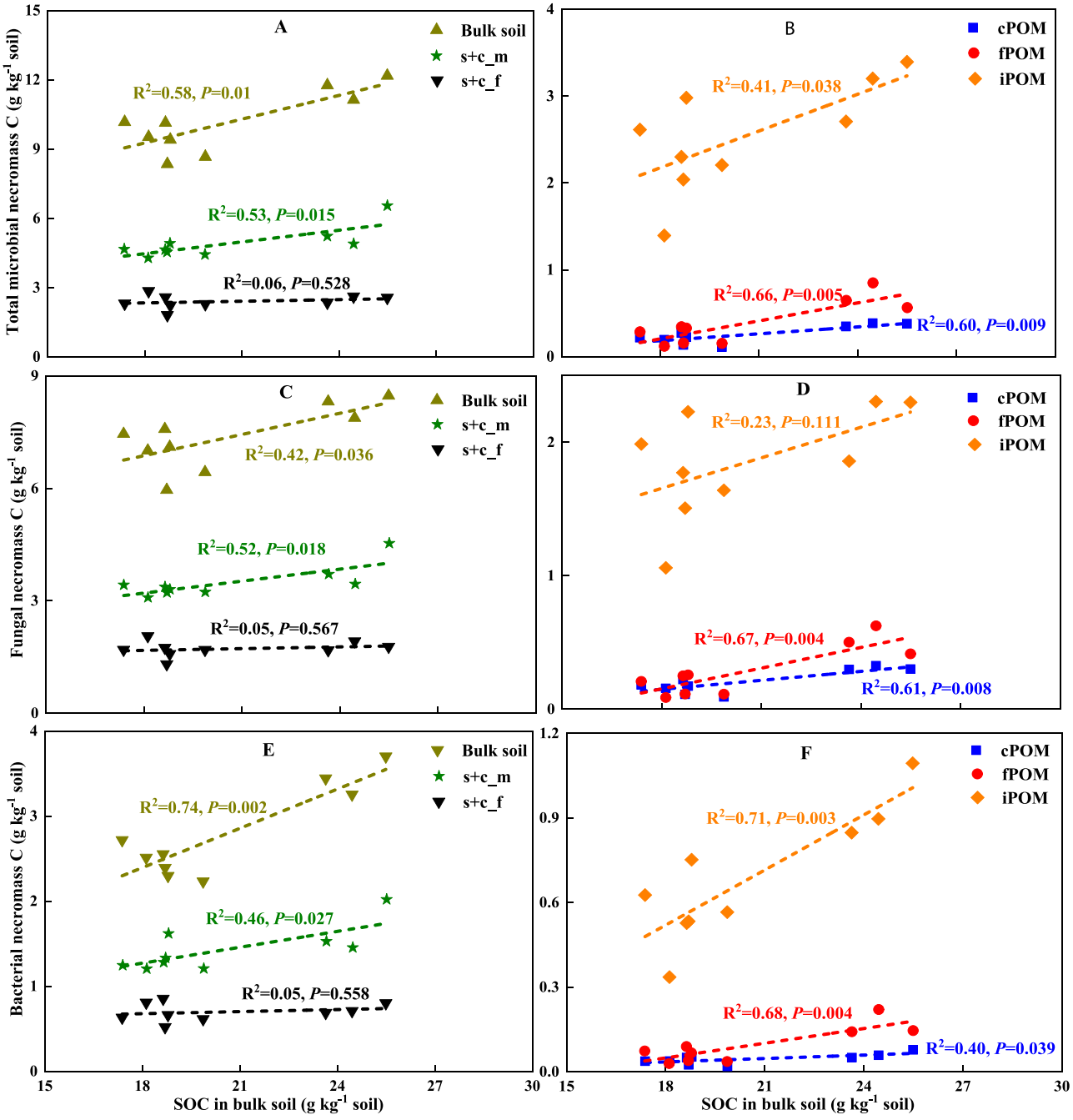

Fig. 5. Linear regression between SOC content in bulk soil and microbial necromass C content in bulk soil and fractions (A-B, total microbial necromass C; C-D, fungal necromass C; E-F, bacterial necromass C).

derived C in POM fractions. The synchronous accumulation of microbial- and plant-derived C resulted in a maintained microbial contribution to SOC in bulk soil and in various fractions under organic fertilization. Overall, our study suggested that the stabilization mechanisms of microbial necromass and its role in SOC sequestration were diverse under different long-term fertilization regimes.

Declaration of Competing Interest

The authors declare that they have no known competing financial interests or personal relationships that could have appeared to influence the work reported in this paper.

Data availability

Data will be made available on request.

Acknowledgements

This study was funded by: Collaborative Innovation Project of Modern Agricultural Research of Jiangxi Province (grant number JXXTCXBSJJ202115); National Engineering and Technology Research Center for Red Soil Improvement (grant number 2020NETRCRSI-5); Basic Research and Talent Training Project of Jiangxi Academy of Agricultural Sciences (grant number JXSNKYJCRC202315); National

Key R&D Program of China (grant number 2017YFD0301601); and Project of Double Thousand Plan in Jiangxi Province of China (grant number jxsq2020102116).

Appendix A. Supplementary data

Supplementary data to this article can be found online at https://doi.org/10.1016/j.geoderma.2023.116688.

References

Adu, J.K., Oades, J.M., 1978. Utilization of organic materials in soil aggregates by bacteria and fungi. Soil Biol. Biochem. 10, 117–122.

Amelung, W., Brodowski, S., Sandhage-Hofmann, A., Bol, R., 2008. Combining biomarker with stable isotope analyses for assessing the transformation and turnover of soil organic matter. Adv. Agro. 100, 155–250.

Angst, G., Mueller, K.E., Nierop, K.G., Simpson, M.J., 2021. Plant-or microbial-derived? A review on the molecular composition of stabilized soil organic matter. Soil Biol. Biochem. 156, 108189.

Appuhn, A., Joergensen, R.G., 2006. Microbial colonisation of roots as a function of plant species. Soil Biol. Biochem. 38, 1040–1051.

Bai, Z., Bodé, S., Huygens, D., Zhang, X., Boeckx, P., 2013. Kinetics of amino sugar formation from organic residues of different quality. Soil Biol. Biochem. 57, 814–821.

Barreiro, A., Bååth, E., Díaz-Raviña, M., 2016. Bacterial and fungal growth in burnt acid soils amended with different high C/N mulch materials. Soil Biol. Biochem. 97, 102–111.

Castellano, M.J., Mueller, K.E., Olk, D.C., Sawyer, J.E., Six, J., 2015. Integrating plant litter quality, soil organic matter stabilization, and the carbon saturation concept. Glob. Chang. Biol. 21, 3200–3209.

Chen, X., Hu, Y., Xia, Y., Zheng, S., Ma, C., Rui, Y., He, H., Huang, D., Zhang, Z., Ge, T., W, J., Guggenberger, G., Kuzyakov, Y., Su, Y., 2021. Contrasting pathways of carbon sequestration in paddy and upland soils. Glob. Change Biol. 27, 2478–2490.

Chen, X., Xia, Y., Hu, Y., Gunina, A., Ge, T., Zhang, Z., Wu, J., Su, Y., 2018. Effect of nitrogen fertilization on the fate of rice residue-C in paddy soil depending on depth: ^{13}C amino sugar analysis. Biol. Fert. Soils 54, 523–531.

Churchman, G.J., 2018. Game changer in soil science. functional role of clay minerals in soil. J. Plant Nutr. Soil Sc. 181, 99–103.

Costa, O.Y.A., Raaijmakers, J.M., Kuramae, E.E., 2018. Microbial extracellular polymeric substances: ecological function and impact on soil aggregation. Front. Microbiol. 9, 1636.

Cotrufo, M.F., Wallenstein, M.D., Boot, C.M., Denef, K., Paul, E., 2013. The microbial efficiency-matrix stabilization (MEMS) framework integrates plant litter decomposition with soil organic matter stabilization: do labile plant inputs form stable soil organic matter? Glob. Chang. Biol. 19, 988–995.

Dai, X., Wang, H., Fu, X., 2017. Soil microbial community composition and its role in carbon mineralization in long-term fertilization paddy soils. Sci. Total Environ. 580, 556–563.

Ding, X., Qiao, Y., Filley, T., Wang, H., Lü, X., Zhang, B., Wang, J., 2017. Long-term changes in land use impact the accumulation of microbial residues in the particle-size fractions of a Mollisol. Biol. Fert. Soils 53, 281–286.

Dong, W.Y., Zhang, X.Y., Dai, X.Q., Fu, X.L., Yang, F.T., Liu, X.Y., Sun, X.M., Wen, X.F., Schaeffer, S., 2014. Changes in soil microbial community composition in response to fertilization of paddy soils in subtropical China. Appl. Soil Ecol. 84, 140–147.

Engelking, B., Flessa, H., Joergensen, R.G., 2007. Shifts in amino sugar and ergosterol contents after addition of sucrose and cellulose to soil. Soil Biol. Biochem. 39, 2111–2118.

Frey, S.D., Lee, J., Melillo, J.M., Six, J., 2013. The temperature response of soil microbial efficiency and its feedback to climate. Nat. Clim. Chang. 3, 395–398.

Glaser, B., Turrión, M.A.B., Alef, K., 2004. Amino sugars and muramic acid—biomarkers for soil microbial community structure analysis. Soil Biol. Biochem. 36, 399–407.

Greenland, D.J., 1971. Interactions between humic and fulvic acidsand clays. Soil Sci. 3, 34–41.

Guggenberger, G., Elliott, E.T., Frey, S.D., Six, J., Paustian, K., 1999. Microbial contributions to the aggregation of a cultivated grassland soil amended with starch. Soil Biol. Biochem. 31, 407–419.

Haddix, M.L., Gregorich, E.G., Helgason, B.L., Janzen, H., Ellert, B.H., Cotrufo, M.F., 2020. Climate, carbon content, and soil texture control the independent formation and persistence of particulate and mineral-associated organic matter in soil. Geoderma 363, 114160.

Harris, K., Young, I.M., Gilligan, C.A., Otten, W., Ritz, K., 2003. Effect of bulk density on the spatial organisation of the fungus Rhizoctonia solani in soil. FEMS Microbiol. Ecol. 44, 45–56.

He, H., Zhang, W., Zhang, X., Xie, H., Zhuang, J., 2011. Temporal responses of soil microorganisms to substrate addition as indicated by amino sugar differentiation. Soil Biol. Biochem. 43, 1155–1161.

Hendrix, P.F., Parmelee, R.W., Crossley, D.A., Coleman, D.C., Odum, E.P., Groffman, P. M., 1986. Detritus food webs in conventional and no-tillage agroecosystems. Bioscience 6, 374–380.

Huang, W., Hall, S.J., 2017. Elevated moisture stimulates carbon loss from mineral soils by releasing protected organic matter. Nat. Commun. 81, 1–10.

Huang, Y., Liang, C., Duan, X., Chen, H., Li, D., 2019. Variation of microbial residue contribution to soil organic carbon sequestration following land use change in a subtropical karst region. Geoderma 353, 340–346.

Huang, S., Rui, W., Peng, X., Huang, Q., Zhang, W., 2010. Organic carbon fractions affected by long-term fertilization in a subtropical paddy soil. Nutr. Cycl. Agroecosys. 86, 153–160.

IUSS Working Group, W.R.B., 2006. World Reference Base for Soil Resources 2006, World Soil Resources Reports No, 1032nd edition. FAO, Rome.

Joergensen, R.G., 2018. Amino sugars as specific indices for fungal and bacterial residues in soil. Biol. Fert. Soils 54, 559–568.

Kögel-Knabner, I., 2002. The macromolecular organic composition of plant and microbial residues as inputs to soil organic matter. Soil Biol. Biochem. 34, 139–162.

Kool, D.M., Chung, H., Tate, K.R., Ross, D.J., Newton, P.C., Six, J., 2007. Hierarchical saturation of soil carbon pools near a natural CO_2 spring. Glob. Chang. Biol. 13, 1282–1293.

Lal, R., 2004. Soil carbon sequestration impacts on global climate change and food security. Science 304, 1623–1627.

Lavallee, J.M., Soong, J.L., Cotrufo, M.F., 2020. Conceptualizing soil organic matter into particulate and mineral-associated forms to address global change in the 21st century. Glob. Chang. Biol. 26, 261–273.

Lehmann, J., Solomon, D., Kinyangi, J., Dathe, L., Wirick, S., Jacobsen, C., 2008. Spatial complexity of soil organic matter forms at nanometre scales. Nat. Geosci. 1, 238–242.

Li, J., Zhang, X., Luo, J., Lindsey, S., Zhou, F., Xie, H., Li, Y., Zhu, P., Wang, L., Shi, Y., He, H., Zhang, X., 2020. Differential accumulation of microbial necromass and plant lignin in synthetic versus organic fertilizer-amended soil. Soil Biol. Biochem. 149, 107967.

Liang, C., 2020. Soil microbial carbon pump: mechanism and appraisal. Soil Ecol. Lett. 2, 241–254.

Liang, C., Schimel, J.P., Jastrow, J.D., 2017. The importance of anabolism in microbial control over soil carbon storage. Nat. Microbiol. 2, 1–6.

Liang, C., Amelung, W., Lehmann, J., Kästner, M., 2019. Quantitative assessment of microbial necromass contribution to soil organic matter. Glob. Chang. Biol. 25, 3578–3590.

Liu, Y., Ge, T., van Groenigen, K.J., Yang, Y., Wang, P., Cheng, K., Zhu, Z., Wang, J., Li, Y., Guggenberger, G., Sardans, J., Penuelas, J., Wu, J., Kuzyakov, Y., 2021a. Rice paddy soils are a quantitatively important carbon store according to a global synthesis. Commun. Earth Environ. 2, 1–9.

Liu, K.L., Huang, J., Li, D.M., Yu, X.C., Ye, H.C., Hu, H.W., Hu, Z.H., Huang, Q.H., Zhang, H.M., 2019. Comparison of carbon sequestration efficiency in soil aggregates between upland and paddy soils in a red soil region of China. J. Integr. Agr. 18, 1348–1359.

Liu, Z., Liu, X., Wu, X., Bian, R., Liu, X., Zheng, J., Zhang, X., Cheng, K., Li, L., Pan, G., 2021b. Long-term elevated CO_2 and warming enhance microbial necromass carbon accumulation in a paddy soil. Biol. Fert. Soils 57, 673–684.

Lu, R., 2000. Analytical methods for soil agricultural chemistry. China Agricultural Science and Technology Press, Beijing, China (in Chinese).

Luan, H., Yuan, S., Gao, W., Tang, J., Li, R., Zhang, H., Huang, S., 2021. Aggregate-related changes in living microbial biomass and microbial necromass associated with different fertilization patterns of greenhouse vegetable soils. Eur. J. Soil Biol. 103, 103291.

Luo, R., Kuzyakov, Y., Liu, D., Fan, J., Luo, J., Lindsey, S., He, J., Ding, W., 2020. Nutrient addition reduces carbon sequestration in a Tibetan grassland soil: disentangling microbial and physical controls. Soil Biol. Biochem. 144, 107764.

Luo, Y., Xiao, M., Yuan, H., Liang, C., Zhu, Z., Xu, J., Kuzyakov, Y., Wu, J., Ge, T., Tang, C., 2021. Rice rhizodeposition promotes the build-up of organic carbon in soil via fungal necromass. Soil Biol. Biochem. 160, 108345.

Murugan, R., Djukic, I., Keiblinger, K., Zehetner, F., Bierbaumer, M., Zechmeister-Bolternstern, S., Joergernsen, R.G., 2019. Spatial distribution of microbial biomass and residues across soil aggregate fractions at different elevations in the Central Austrian Alps. Geoderma 339, 1–8.

Neely, C.L., Beare, M.H., Hargrove, W.L., Coleman, D.C., 1991. Relationships between fungal and bacterial substrate-induced respiration, biomass and plant residue decomposition. Soil Biol. Biochem. 23, 947–954.

Rousk, J., Brookes, P.C., Bååth, E., 2009. Contrasting soil pH effects on fungal and bacterial growth suggest functional redundancy in carbon mineralization. Appl. Environ. Microb. 75, 1589–1596.

Schlüter, S., Roussety, T., Rohe, L., Guliyev, V., Blagodatskaya, E., Reitz, T., 2022. Land use impact on carbon mineralization in well aerated soils is mainly explained by variations of particulate organic matter rather than of soil structure. Soil 8, 253–267.

Schmidt, J., Schulz, E., Michalzik, B., Buscot, F., Gutknecht, J.L., 2015. Carbon input and crop-related changes in microbial biomarker levels strongly affect the turnover and composition of soil organic carbon. Soil Biol. Biochem. 85, 39–50.

Schneider, M.P.W., Scheel, T., Mikutta, R., Hees, P.V., Kalbitz, K., 2010. Sorptive stabilization of organic matter by amorphous al hydroxide. Geochim. Cosmochim. AC. 74, 1606–1619.

Sey, B.K., Manceur, A.M., Whalen, J.K., Gregorich, E.G., Rochette, P., 2008. Small-scale heterogeneity in carbon dioxide, nitrous oxide and methane production from aggregates of a cultivated sandy-loam soil. Soil Biol. Biochem. 40, 2468–2473.

Six, J., Elliott, E.T., Paustian, K., Doran, J.W., 1998. Aggregation and soil organic matter accumulation in cultivated and native grassland soils. Soil Sci. Soc. Am. J. 62, 1367–1377.

Six, J., Callewaert, P., Lenders, S., De Gryze, S., Morris, S.J., Gregorich, E.G., Paul, E.A., Paustian, K., 2002a. Measuring and understanding carbon storage in afforested soils by physical fractionation. Soil Sci. Soc. Am. J. 66, 1981–1987.

Six, J., Conant, R.T., Paul, E.A., Paustian, K., 2002b. Stabilization mechanisms of soil organic matter: implications for C-saturation of soils. Plant and Soil 241, 155–176.
Sokol, N.W., Sanderman, J., Bradford, M.A., 2018. Pathways of mineral-associated soil organic matter formation: Integrating the role of plant carbon source, chemistry, and point of entry. Glob. Chang. Biol. 25, 12–24.
Stewart, C.E., Plante, A.F., Paustian, K., Conant, R.T., Six, J., 2008. Soil carbon saturation: linking concept and measurable carbon pools. Soil Sci. Soc. Am. J. 72, 379–392.
Stewart, C.E., Paustian, K., Conant, R.T., Plante, A.F., Six, J., 2009. Soil carbon saturation: Implications for measurable carbon pool dynamics in long-term incubations. Soil Biol. Biochem. 41, 357–366.
Tong, X., Xu, M., Wang, X., Bhattacharyya, R., Zhang, W., Cong, R., 2014. Long-term fertilization effects on organic carbon fractions in a red soil of China. Catena 113, 251–259.
von Lützow, M., Kögel-Knabner, I., Ludwig, B., Matzner, E., Flessa, H., Ekschmitt, K., Guggenberger, G., Marschner, B., Kalbitz, K., 2008. Stabilization mechanisms of organic matter in four temperate soils: Development and application of a conceptual model. J. Plant Nutr. Soil Sc. 171, 111–124.
Wang, B., An, S., Liang, C., Liu, Y., Kuzyakov, Y., 2021. Microbial necromass as the source of soil organic carbon in global ecosystems. Soil Biol. Biochem. 162, 108422.
Wang, C., Wang, X., Pei, G., Xia, Z., Peng, B., Sun, L., Wang, J., Gao, D., Chen, S., Liu, D., Dai, W., Jiang, P., Fang, Y., Liang, C., Wu, N., Bai, E., 2020. Stabilization of microbial residues in soil organic matter after two years of decomposition. Soil Biol. Biochem. 141, 107687.
Wei, L., Ge, T., Zhu, Z., Ye, R., Penuelas, J., Li, Y., Lynn, T.M., Jones, D.L., Wu, J., Kuzyakov, Y., 2022. Paddy soils have a much higher microbial biomass content than upland soils: A review of the origin, mechanisms, and drivers. Agr Ecosyst Environ 326, 107798.
Wiesmeier, M., Urbanski, L., Hobley, E., Lang, B., von Lützow, M., Marin-Spiotta, E., van Wesemael, B., Rabot, E., Ließ, M., Garcia-Franco, N., Wollschläger, U., 2019. Soil organic carbon storage as a key function of soils-A review of drivers and indicators at various scales. Geoderma 333, 149–162.
Xia, Y., Chen, X., Zheng, S., Gunina, A., Ning, Z., Hu, Y., Tang, H., Rui, Y., Zhang, Z., He, H., Huang, D., Su, Y., 2021. Manure application accumulates more nitrogen in paddy soils than rice straw but less from fungal necromass. Agr Ecosyst Environ 319, 107575.
Xu, S., Shi, X., Zhao, Y., Yu, D., Li, C., Wang, S., Tan, M., Sun, W., 2011. Carbon sequestration potential of recommended management practices for paddy soils of China, 1980–2050. Geoderma 166, 206–213.
Yan, M., Zhang, X., Liu, K., Lou, Y., Wang, Y., 2022. Particle size primarily shifts chemical composition of organic matter under long-term fertilization in paddy soil. Eur. J. Soil Sci. 73, e13170.
Yan, X., Zhou, H., Zhu, Q.H., Wang, X.F., Zhang, Y.Z., Yu, X.C., Peng, X., 2013. Carbon sequestration efficiency in paddy soil and upland soil under long-term fertilization in southern China. Soil Tillage Res. 130, 42–51.
Yang, F., Tian, J., Meersmans, J., Fang, H., Yang, H., Lou, Y., Li, Z., Liu, K., Zhou, Y., Blagodatskaya, E., Kuzyakov, Y., 2018. Functional soil organic matter fractions in response to long-term fertilization in upland and paddy systems in South China. Catena 162, 270–277.
Ye, G., Lin, Y., Kuzyakov, Y., Liu, D., Luo, J., Lindsey, S., Wang, W., Fan, J., Ding, W., 2019. Manure over crop residues increases soil organic matter but decreases microbial necromass relative contribution in upland Ultisols: Results of a 27-year field experiment. Soil Biol. Biochem. 134, 15–24.
Zhang, X., Amelung, W., 1996. Gas chromatographic determination of muramic acid, glucosamine, mannosamine, and galactosamine in soils. Soil Biol. Biochem. 28, 1201–1206.
Zhang, X., Wang, Y., Wen, J., Zhang, Y., Zeng, X., 2021. The C/N ratio and phenolic groups of exogenous dissolved organic matter together as an indicator for evaluating the stability of mineral-organic associations in red soil. J. Soil. Sediment. 21, 1–11.